THE JOURNAL OF PHYSICAL CHEMISTRY B

Article

pubs.acs.org/JPCB

Effect of High Exogenous Electric Pulses on Protein Conformation: Myoglobin as a Case Study

Paolo Marracino,[†] Francesca Apollonio,[†] Micaela Liberti,[†] Guglielmo d'Inzeo,[†] and Andrea Amadei*[,‡]

[†]Dipartimento di Ingegneria dell'Informazione, Elettronica e Telecomunicazioni Sapienza, Università di Roma, Roma, Italy

[‡]Dipartimento di Scienze e Tecnologie Chimiche, Università di Roma 'Tor Vergata', Roma, Italy

ABSTRACT: Protein folding and unfolding under the effect of exogenous perturbations remains a topic of great interest, further enhanced by recent technological developments in the field of signal generation that allow the use of intense ultrashort electric pulses to directly interact at microscopic level with biological matter. In this paper, we show results from molecular dynamics (MD) simulations of a single myoglobin molecule in water exposed to pulsed and static electric fields, ranging from 10^8 to 10^9 V/m, compared to data with unexposed conditions. We have found that the highest intensity (10^9 V/m) produced a fast transition (occurring within a few hundreds of picoseconds) between folded and unfolded states, as inferred by secondary structures and geometrical analysis. Fields of 10^8 V/m, on the contrary, produced no significant denaturation, although a relevant effect on the protein dipolar behavior was detected.

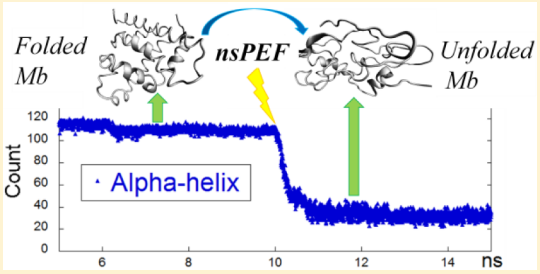

INTRODUCTION

Under physiological conditions, a protein spends most of its lifetime in the native conformation, although this represents only a small part of its available configurational space. Endogenous and exogenous perturbations acting on the protein can alter the thermodynamic equilibrium of the system, leading to a transition toward the denaturated state, with kinetics depending on the characteristics and intensities of the stimuli.

Several works have experimentally and theoretically treated a set of exogenous perturbations, as temperature,[1−5] pressure,[4−7] pH changes,[8] mechanical forces,[9] laser excitation,[10] and chemical agents[11] acting on folding and unfolding processes of a wide number of proteins. Despite such extensive literature, the details of these processes at an atomic level have proved to be elusive both to traditional experimental approaches and to theoretical methods based on macroscopic or mesoscopic models. Therefore, many authors in the recent past have presented full atomistic simulation studies of mechanical, thermal, electric, and even electromagnetic stress response of prototype proteins and peptides.[12−21] In particular, the effect of electric (E) and electromagnetic (EM) fields showed a strong evidence of changes in protein secondary structure and disruption of hydrogen bonds associated with protein charged residues, for intensities higher than 5×10^8 V/m,[22−24] indicating the coupling between protein structure and high intense electric fields.

The reason behind our interest in electric field effects on protein thermodynamics and conformation relies on recent results and future trends that exploit electric pulse stimuli. These results have not yet been as thoroughly considered, despite their unique potential, and may represent clear opportunities for advancing in biomedical fields.[25] In particular, the use of pulse trains with a time length of nanoseconds and intensities on the order of tens of MV/m, named nanosecond pulsed electric fields (nsPEFs),[26,27] seems to indicate that such pulses induce apoptosis and cause loss of vascular viability contributing to infarctive tumor death in a temperature-independent manner.[26] Since nsPEFs directly affect cellular substructures and proteins in both the cytoplasm and the extracellular environment,[28] a possible apoptosis pathway could be linked to the endoplasmic reticulum (ER) stress, due to the activation of the unfolded protein response (UPR), a homeostatic signaling network that orchestrates the recovery of the ER function, and failure to adapt to ER stress resulting in apoptosis.[29,30] Moreover, several authors[31−33] have shown that nsPEFs can kill tumor cells in culture by triggering cell suicide: the interaction mechanism exerted does not involve thermal effects, but it may lead to multiple apoptosis pathways such as the cytochrome *c* release or the activation of caspase enzymes.

Some authors, until recently, have been trying to elucidate the interaction between nsPEFs and biological membranes in order to understand the mechanism of pore formation and stability.[34,35] Given the characteristic time length associated with a typical nsPEF signal, molecular dynamics (MD) simulations seem to be the perfect tool to study conformational and thermodynamic changes induced by the field on biological structures. In this context, in order to give a contribution in comprehending the mechanism of molecular interaction of nsPEF, we chose to study the unfolding process of a protein. As a case study, we have selected myoglobin (Mb), which has been

Received: October 5, 2012
Revised: January 15, 2013

   dx.doi.org/10.1021/jp309857b | *J. Phys. Chem. B* XXXX, XXX, XXX−XXX

the first globular protein whose structure was worked out from X-ray diffraction by protein crystals. Mb is probably one of the most simulated proteins, which long served as a model system for investigating ligand binding,[36,37] migration,[38] and conformational relaxation in proteins,[39,40] even under the effect of exogenous electromagnetic field stimuli.[41] At the same time, several experimental and theoretical works involving Mb are present in the literature,[42−48] nonetheless, to our knowledge, the present work represents the first attempt to rigorously characterize a system containing a Mb protein in water under the effect of nsPEFs by means of classical MD simulations.

THEORETICAL METHODS

We carried out MD simulations of myoglobin in water using the GROMACS package.[49] The simulated system consisted of a rectangular box (around 6 nm side), where we placed a single myoglobin and 6740 single point charge (SPC)[50] water molecules resulting in a typical density of 1000 kg/m^3. Note that, to properly describe myoglobin physiological behavior, it was necessary to simulate a box of water molecules large enough to reproduce both the first hydration shells and a significant amount of bulk water. The myoglobin is made of 153 residues and the heme group (the overall charge of the system is zero). Following an energy minimization and subsequent solvent relaxation, the system was gradually heated from 50 to 300 K using short (typically 60 ps) MD simulations. A first trajectory was propagated up to 50 ns in the NVT ensemble using an integration step of 2 fs and removing the myoglobin center of mass translation but with no constraints on its related rotation. The temperature was kept constant at 300 K by the Berendsen thermostat[51] with the relaxation time (τ) equal to the simulation time step, hence virtually equivalent to the isothermal coupling[52] which provides consistent statistical mechanical behavior. All bond lengths were constrained using LINCS algorithm.[53] Long-range electrostatics were computed by the particle mesh Ewald method[54] with 34 wave vectors in each dimension and a fourth-order cubic interpolation. The ffG43a1 force field[55] parameters were adopted. Once an exhaustive equilibrated-unexposed trajectory was obtained, we evaluated possible effects induced by a high exogenous electric field, hence introducing two different E field signals, a pulsed and a static (constant) one (see Table 1), each with two different intensities of 10^9 and 10^8 V/m, acting in the simulation box as explained in ref 41. More precisely, the application of the electric field takes place in continuity at the last frame of the unexposed simulation, thus allowing a direct evaluation of the characteristic response over time of the system due to the switching of the exogenous perturbation.

Table 1. Summary of Simulated Systems

exposure condition	E field intensity (V/m)	pulse duration (ns)	simulation length (ns)
static #1 (constant E field)	10^9		100
pulsed #1	10^9	8	118
static #2 (constant E field)	10^8		50
pulsed #2	10^8	8	68
ref	0		50

A simple method to characterize the geometry of a complex system like a protein is to approximate its overall geometrical structure, at each MD frame, to the ellipsoid given by the eigenvectors of the covariance matrix as obtained by the distribution of the x, y, and z coordinates of the protein atoms (the geometrical matrix $\tilde{C}$). Therefore, for a system defined by N atoms, the elements of the 3 × 3 geometrical matrix at each time frame are given by

$$\tilde{C} = \frac{1}{N}\sum_{l=1}^{N}(\mathbf{r}_l - \langle\mathbf{r}\rangle)(\mathbf{r}_l - \langle\mathbf{r}\rangle)^T \quad (1)$$

where $\mathbf{r}_l$ is the l-th atom position vector and $\langle\mathbf{r}\rangle$ is the mean atomic position vector as obtained by averaging all of the atom position vectors. Diagonalization of the geometrical matrix provides three eigevectors ($\boldsymbol{c}_i$, i = 1, 2, 3) corresponding to the three axes of the ellipsoid best fitting the atom distribution at that MD time frame (geometrical axes) and three corresponding eigenvalues (λ_i, i = 1, 2, 3) given by the mean square fluctuations of the atomic positions along each eigenvector and providing the size of the ellipsoid along its axes.

Finally, in order to assess possible effects induced on the secondary structure of the myoglobin, we used the DSSP program[56] to calculate the secondary structure time evolution along the MD trajectory.

RESULTS AND DISCUSSION

Geometrical Properties. In order to identify the possible effects of high exogenous electric fields on protein geometry, in Figure 1, we present a direct comparison of myoglobin geometrical matrix eigenvalues under different exposure conditions.

As a reference condition, we have taken into account the 50 ns unexposed trajectory, obtaining the time course of the three geometrical matrix eigenvalues (Figure 1a). Their relative average magnitude of about 3.7:2.7:1 indicates an overall compact globular shape of the myoglobin protein, lasting for the whole simulation length. The application of a rectangular pulse with a null rise time and intensity of 10^9 V/m (Figure 1b) produces a fast and marked structural rearrangement occurring within a few hundred picoseconds mainly along the myoglobin major geometrical axis. Note that after the electric field pulse switch off myoglobin essentially stands in its new geometry with no appreciable relaxation to its physiological state, hence indicating that high intensity electric pulses with a duration of a few nanoseconds suffice to produce a fast irreversible transition (at least within the time length considered). This finding is strengthened considering that the application of a static 10^9 V/m electric field produces the same geometry of the few nanoseconds pulse (see Figure 1c) condition. This is also shown in Figure 2, where we present the normalized distributions of the myoglobin major geometrical eigenvalue clearly indicating that the protein, under the effect of both the pulsed and the static E field, is essentially stable in a well-defined geometrical state, which is rather different from the one of the reference unexposed condition.

Secondary Structure Analysis. We decided to evaluate the possible effect induced by the exogenous field on myoglobin secondary structures. Crystallographic data assessed that almost 70% of the polypeptide is α-helical, with the presence of other secondary structure elements such as turn, coil and bend. In Figure 3, the time course of these secondary structure elements is shown for the 10^9 V/m nsPEF simulation (pulsed #1; see Table 1), around the instant of the onset of the electric pulse (in continuity with the unexposed trajectory) to better understand possible effects induced by the electric field

dx.doi.org/10.1021/jp309857b | J. Phys. Chem. B XXXX, XXX, XXX−XXX

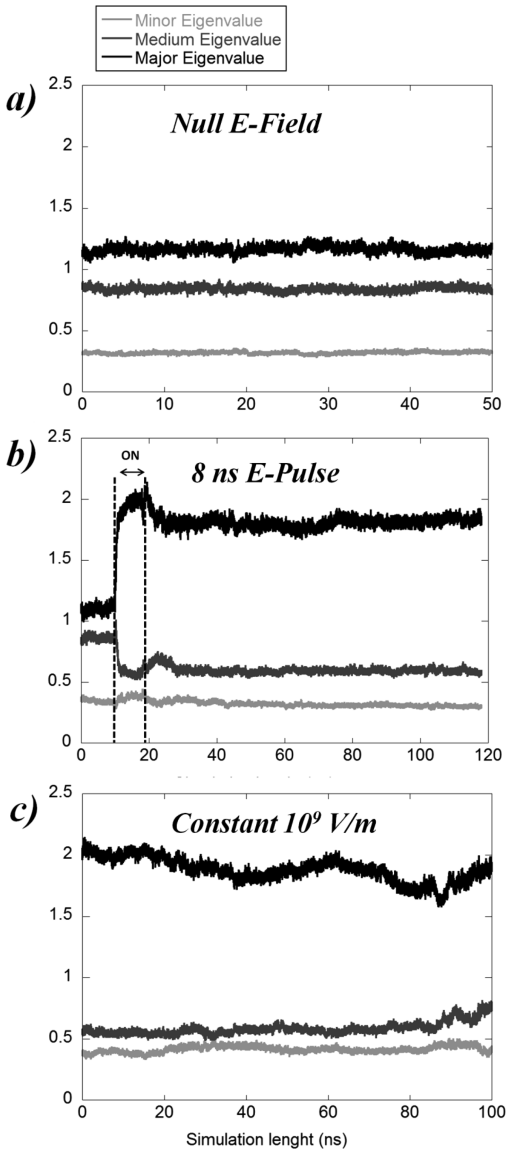

Figure 1. Time course of the three eigenvalues from the diagonalization of the geometrical matrix: (a) equilibrium behavior for the unexposed system of the three eigenvalues. (b,c) Corresponding time courses in the presence of the E field pulsed or static perturbation, respectively.

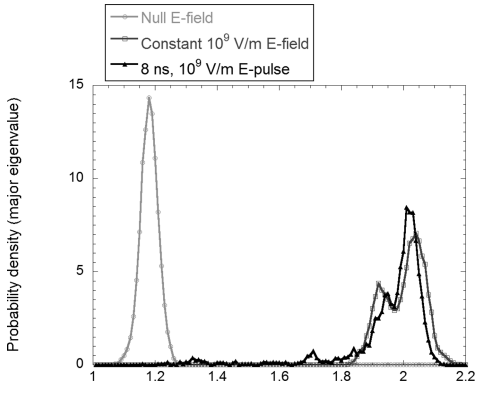

Figure 2. Probability distributions of myoglobin major geometrical eigenvalue for the reference (light gray circles), nsPEF (black triangles), and constant E field exposure (gray squares) conditions.

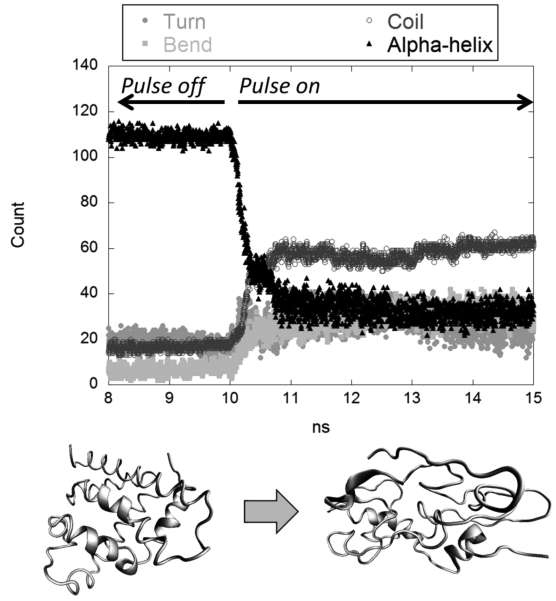

Figure 3. Time course of the amount (in residues) of relevant secondary structure elements nearby the electric pulse application. The 10^9 V/m nsPEF is able to induce the disruption of about 70% of the α-helix elements (black triangles) within 1 ns after the pulse switch on. The other secondary structure elements experience a similar behavior. Below, two snapshots of the folded (left) and unfolded (right) conformations are provided: note that myoglobin structure is significantly stretched along the Cartesian x-axis (i.e., the direction of the exogenous electric field).

just after the pulse application. It is worth noting that, within 1 ns, a severe disruption of the α-helix elements is observed, coupled to a fast increase of turn, coil, and bend elements, indicating an unfolding transition. There are two questions arising from these latter results: (a) Is a nsPEF sufficient to induce an essentially irreversible (within several tens of nanoseconds) protein unfolding? (b) Does a static electric field quantitatively produce the same results? Data shown in Figure 4 provide evidence to answer these questions.

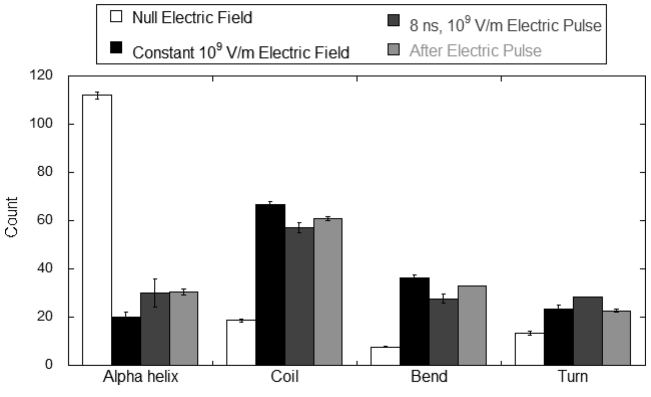

Figure 4. Amount of residues of secondary structure elements considered relevant to define the folded and unfolded states. Both 10^9 V/m static and nsPEF perturbations produce a sharp decrease in α-helix amount. For the other secondary structure elements considered, we observe, as expected, a complementary behavior. The error bars were obtained by calculating the standard error using five different portions of the total equilibrium trajectories. For the non-equilibrium case (pulsed #1 in Table 1), the standard error has been evaluated by performing three independent simulations.

dx.doi.org/10.1021/jp309857b | J. Phys. Chem. B XXXX, XXX, XXX−XXX

Histograms of the secondary structure elements for the unexposed and exposed systems are shown, with a clear indication of myoglobin response during and after the nsPEF application. From the figure, it is possible to appreciate the irreversible effect on protein secondary structure induced by both static and pulsed E fields, lasting, for the latter, even after the pulse switch off at least within the simulation time length (several tens of nanoseconds).

Dipole Moment Dynamics and Distribution. A simple measure of the effects of an external electric field on protein behavior is, of course, the protein polarization response to the field exposure. Since we are interested in the field effects on protein internal behavior rather than the trivial reorientation of the whole protein (i.e., rotational effects), we consider the protein dipole moment expressed in the internal Cartesian reference of frame given by the three geometrical axes and centered in the protein center of mass. In this way, any relevant variation of the dipole moment can be directly considered as a transition of the protein structural/conformational regime and hence utilized to investigate the protein functional response to the applied field.

In Figure 5, we present the time course of the protein dipole moment vector for different exposure conditions. Comparison between panels a and b shows how the nsPEF induces, just after its application, a fast transition of the dipole moment along the major geometrical axis, leaving the other components unchanged. The transition, similarly to the other observables considered, reaches a steady state within a few hundred picoseconds and, interestingly, after the pulse switch off, the system does not fully relax toward the physiological state but it remains significantly polarized. Not surprisingly, when we consider a static E field acting on Mb (panel c), the dipole moment along the major geometrical axis remains essentially constant at a high value identical to the one reached during the pulse, while, again, the other components remain unchanged with respect to the unexposed condition.

Finally, in Figure 6, we show the normalized distributions of the dipole moment along the major geometrical axis for the reference unexposed condition and the two exposure conditions. The figure clearly confirms the dramatic transition induced by the field exposure and the very similar behavior of the exposed conditions, pointing out that nsPEFs of a few nanoseconds with a 10^9 V/m intensity suffice to produce essentially the same effect of a static electric perturbation of the same intensity.

Effect of Lower Electric Fields. Up to now, we have discussed data obtained with an intensity of the exogenous field of 10^9 V/m, comparing results with the reference unexposed simulation. The effects induced by such an external stimulus are clear, embracing geometrical shifts, secondary structure rearrangement, and sharp polarization effects. As presented in Table 1, we have performed further simulations with a lower intensity of the exogenous electric field, 10^8 V/m, that is the intensity used in recent computational works.[21−24] We analyzed the same observables previously considered, obtaining no significant effects of the exogenous field on geometric and secondary structure properties (data not shown), hence indicating no unfolding transitions in our simulations. Nonetheless, this lower intensity electric field affects the myoglobin dipole moment, as shown in Figure 7, where we report the dipole moment along the geometrical axes as a function of the time interval starting when the exogenous 10^8 V/m electric fields have been switched on. From the figure, it is evident that

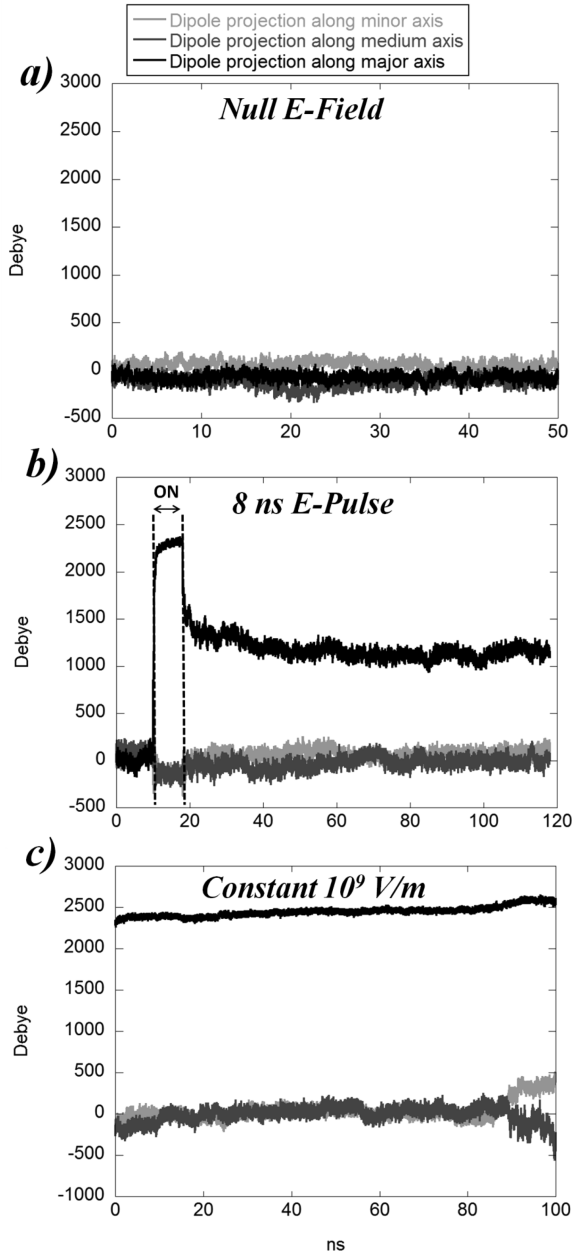

Figure 5. Time courses of myoglobin dipole moment projected along the three protein geometrical axes. (a) Reference unexposed simulation; (b) 10^9 V/m nsPEF simulation; (c) 10^9 V/m static electric field simulation.

the dipole transition occurs within 20 ns, hence corresponding to a much slower kinetics when compared to the corresponding transition occurring when a 10^9 V/m exogenous E field is used (see Figure 5b). In Figure 8, we also show, for the three dipole components along the geometrical axes, the corresponding equilibrium probability distributions obtained by the simulation with the static 10^8 V/m exogenous E field, again clearly showing a significant effect in these equilibrium distributions, resulting in similar shifts of the dipole mean values. Such polarization along the axes of the *internal* reference of frame, that is, the three geometrical axes, clearly indicates a sort of structural rearrangement which alters neither the overall geometrical shape nor the secondary structures of the protein. Such a structural transition associated with the enhanced polarization of myoglobin is actually essentially given by the

dx.doi.org/10.1021/jp309857b | J. Phys. Chem. B XXXX, XXX, XXX−XXX

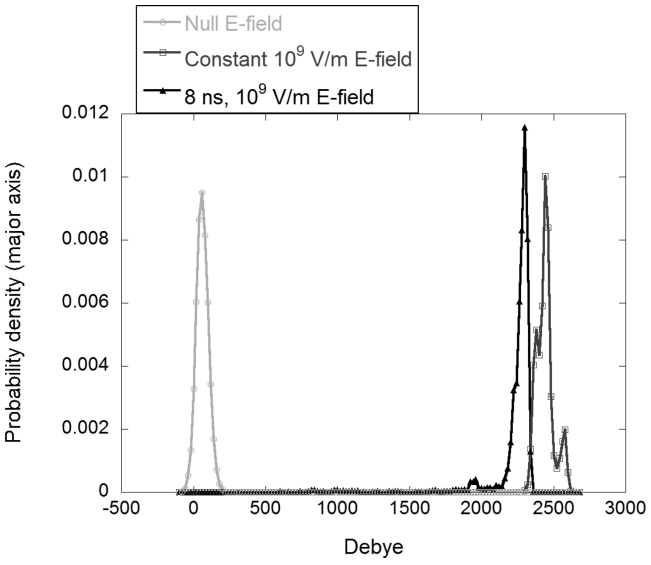

Figure 6. Probability distributions of myoglobin dipole moment projected along the myoglobin major geometrical axis, for the unexposed simulation (light gray circles) and in the presence of the 109 V/m pulsed (black triangles) and static (gray squares) electric fields.

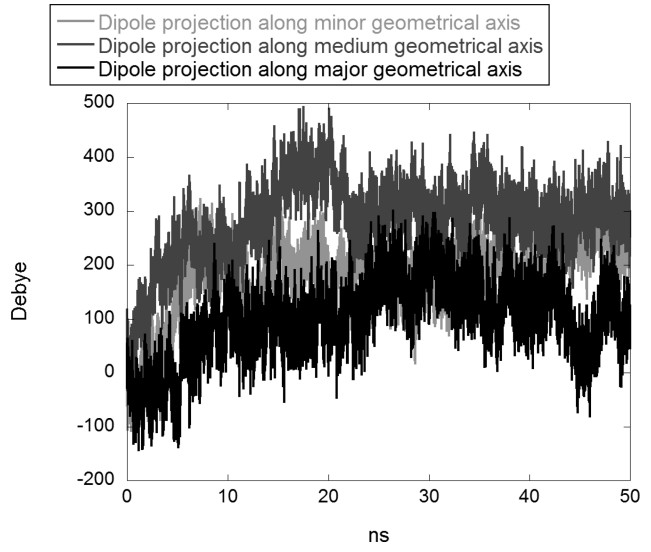

Figure 7. Time course of myoglobin dipole moment projected along the three protein geometrical axes. The time interval starts when the 10^8 V/m exogenous field has been switched on.

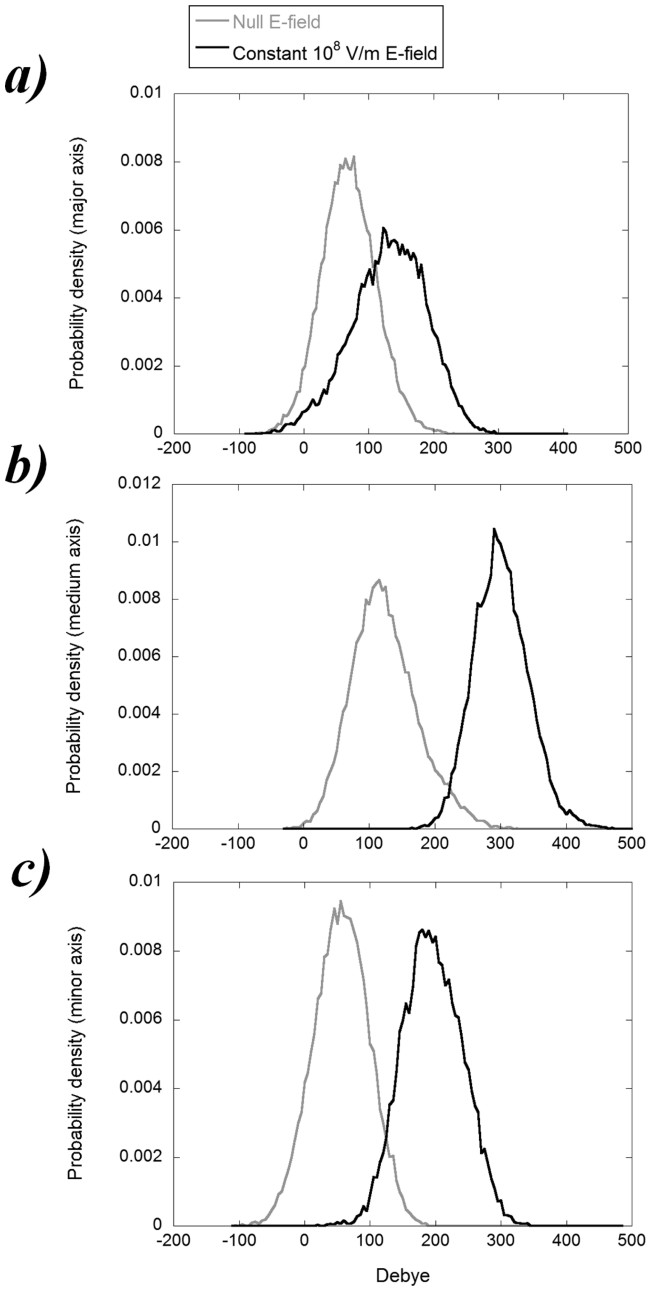

Figure 8. Equilibrium probability distributions of myoglobin dipole moment projected along myoglobin major geometrical axis (a), medium axis (b), and minor axis (c) in the presence of a 10^8 V/m static electric field.

stretching of the N-terminal to carboxy-terminal distance due to the interaction of the exogenous electric field with the end-to-end dipole.

CONCLUSIONS

In this paper, we used solvated Mb to investigate in detail structural conformational effects due to applied exogenous electric fields, in order to characterize the response of the protein (e.g., its folding−unfolding transitions and, more in general, the changes of protein behavior). Our results based on extended MD simulations (50 ns for the null and the lower field and up to 100 ns for the higher field) allowed the evaluation of the relaxation and equilibrium properties for the three cases studied: the null field, 10^8 V/m, and 10^9 V/m pulsed or static fields conditions. We found that with a 10^9 V/m applied exogenous E field myoglobin undergoes a fast unfolding transition (occurring within 100−200 ps) characterized by a very intense polarization with respect to the reference null field condition, which in turn is the cause of the denaturation. On the other hand, when using a 10^8 V/m applied exogenous electric field, although a significant increase of polarization with respect to the null field condition is still present, no appreciable denaturation within our simulations (50 ns) can be detected. Such a structural rearrangement (occurring within 10−20 ns from the field switch on) associated with a relevant change of the protein polarization essentially due to the protein end-to-end distance increase does not provide any significant alteration of both the overall geometrical shape (see Table 2) and

dx.doi.org/10.1021/jp309857b | J. Phys. Chem. B XXXX, XXX, XXX−XXX

Table 2. Geometrical Properties of Myoglobin under Different Exposure Conditions[a]

exposure condition	E field intensity (V/m)	$\langle c^2_{major,x}\rangle$	$\langle c^2_{medium,x}\rangle$	$\langle c^2_{minor,x}\rangle$	$2\sqrt{\lambda_{major}}$	V_{ellips}
static #1 (constant E field)	10^9	0.99 ± 0.002	0.002 ± 0.0007	0.002 ± 0.001	2.83 ± 0.02	22.27 ± 0.22
pulsed #1	10^9	0.98 ± 0.002	0.04 ± 0.02	0.006 ± 0.002	2.77 ± 0.05	23.5 ± 1.3
static #2 (constant E field)	10^8	0.19 ± 0.03	0.53 ± 0.04	0.27 ± 0.03	2.12 ± 0.01	18.62 ± 0.07
pulsed #2	10^8	0.36	0.43	0.20	2.14	18.61
ref	0	0.38 ± 0.09	0.34 ± 0.09	0.27 ± 0.1	2.15 ± 0.01	18.7 ± 0.06

[a]The $\langle c^2_{major,x}\rangle$, $\langle c^2_{medium,x}\rangle$, and $\langle c^2_{minor,x}\rangle$ represent the mean square x-components of the myoglobin geometrical eigenvectors indicating the presence of favored rotational orientations due to presence of the exogenous electric field aligned along the x-axis (for a freely tumbling molecule, these mean values should be 1/3); $2\sqrt{\lambda_{major}}$ term represents a measure of the myoglobin geometrical major semi-axis (within 95% of probability); V_{ellips} is the volume of the ellipsoid approximating myoglobin geometry given by the three geometrical semi-axes via $^4/_3\pi(8(\lambda_{major}\lambda_{medium}\lambda_{minor})^{1/2})$. When indicated, the noise corresponds to the standard error.

secondary structures (see Table 3). Note that from Table 2 it is evident that at high applied field the protein unfolding is

Table 3. Protein−Protein and Protein−Solvent Mean Number of Hydrogen Bonds at Different Exposure Conditions (When Indicated, the Noise Corresponds to the Standard Error)

exposure condition	E field intensity (V/m)	H_{bonds}(protein−protein)	H_{bonds}(protein−solvent)
static #1 (constant E field)	10^9	76.05 ± 1.15	323.43 ± 2.69
pulsed #1	10^9	79.07 ± 2.01	327.50 ± 1.6
static #2 (constant E field)	10^8	124.28 ± 0.77	274.37 ± 1.77
pulsed #2	10^8	123.27	277.56
ref	0	122.28 ± 0.23	279.21 ± 0.9

associated with a relevant geometrical rearrangement leading to the overlapping between the unfolded protein dipole (essentially given by the end-to-end distance vector) and the major geometrical axis (this is evidenced by the fact that the major geometrical axis is almost perfectly aligned along the exogenous electric field direction, i.e., the laboratory reference of frame). On the contrary, at the lower electric field intensity, where no protein unfolding occurs, the native protein dipole is roughly aligned along the medium geometrical axis (see Figure 7), which results to be the best aligned along the laboratory reference of frame x-axis. Our data clearly indicate that the critical exogenous electric field able to induce a significant unfolding process must be between 10^8 and 10^9 V/m, in agreement with previous literature results on different protein−peptide molecules.[21−24] Lower applied exogenous E fields, although unable to promote unfolding transitions, at least within the simulation times sampled, may relevantly polarize the protein molecule via subtle structural changes. Finally, it is worth remarking that the present study, as well as the few other theoretical−computational studies in literature on the same subject, provides qualitative and quantitative information to properly understand the interaction mechanisms between biological macromolecules and pulsed or static electric fields, promising to furnish important data for both biomedical and nanotechnological application.

AUTHOR INFORMATION

Corresponding Author

*E-mail: andrea.amadei@uniroma2.it.

Notes

The authors declare no competing financial interest.

REFERENCES

(1) Baldwin, R. L. Temperature Dependence of the Hydrophobic Interaction in Protein Folding. *Proc. Natl. Acad. Sci. U.S.A.* **1986**, *83*, 8069−8072.
(2) Baldwin, R. L.; Muller, N. Relation between the Convergence Temperatures Th* and Ts* in Protein Unfolding. *Proc. Natl. Acad. Sci. U.S.A.* **1992**, *89*, 7110−7113.
(3) Day, R.; Brian, J.; Bennion, B. J.; Ham, S.; Daggett, V. Increasing Temperature Accelerates Protein Unfolding without Changing the Pathway of Unfolding. *J. Mol. Biol.* **2002**, *322*, 189−203.
(4) Hawley, S. A. Reversible Pressure-Temperature Denaturation of Chymotrypsinogen. *Biochemistry* **1971**, *10*, 2436−2442.
(5) Wiedersich, J.; Köhler, S.; Skerra, A.; Friedrich, J. Temperature and Pressure Dependence of Protein Stability: The Engineered Fluorescein-Binding Lipocalin FluA Shows an Elliptic Phase Diagram. *Proc. Natl. Acad. Sci. U.S.A.* **2008**, *105*, 5756−5761.
(6) Panick, G.; Malessa, R.; Winter, R.; Rapp, G.; Frye, K. G.; Royer, C. A. Structural Characterization of the Pressure-Denatured State and Unfolding/Refolding Kinetics of Staphylococcal Nuclease by Synchrotron Small-Angle X-ray Scattering and Fourier-Transform Infrared Spectroscopy. *J. Mol. Biol.* **1998**, *275*, 389−402.
(7) Hummer, G.; Garde, S.; García, A. E.; Paulaitis, M. E.; Pratt, L. R. The Pressure Dependence of Hydrophobic Interactions Is Consistent with the Observed Pressure Denaturation of Proteins. *Proc. Natl. Acad. Sci. U.S.A.* **1998**, *95*, 1552−1555.
(8) Shen, L. L.; Hermans, J. Kinetics of Conformation Change of Sperm-Whale Myoglobin. I. Folding and Unfolding of Metmyoglobin Following pH Jump. *Biochemistry* **1972**, *11*, 1836−1841.
(9) Rief, M.; Gautel, M.; Oesterhelt, F.; Fernandez, J. M.; Gaub, H. E. Reversible Unfolding of Individual Titin Immunoglobulin Domains by AFM. *Science* **1997**, *276*, 1109−1112.
(10) Jones, C. M.; Henry, E. R.; Hu, Y.; Chan, C.; Luck, S. D.; Bhuyan, A.; Roder, H.; Hofrichter, J.; Eaton, W. A. Fast Events in Protein Folding Initiated by Nanosecond Laser Photolysis. *Proc. Natl. Acad. Sci. U.S.A.* **1993**, *90*, 11860−11864.
(11) Scholtz, J. M.; Barrick, D.; York, E. J.; Stewart, J. M.; Baldwin, R. L. Urea Unfolding of Peptide Helices as a Model for Interpreting Protein Unfolding. *Proc. Natl. Acad. Sci. U.S.A.* **1995**, *92*, 185−189.
(12) Laurence, J. A.; French, P. W.; Lidner, R. A.; McKenzie, D. R. Biological Effects of Electromagnetic Fields: Mechanisms for the Effects of Pulsed Microwave Radiation on Protein Conformation. *J. Theor. Biol.* **2000**, *206*, 291−298.
(13) Adair, R. K. Vibrational Resonances in Biological Systems at Microwave Frequencies. *Biophys. J.* **2002**, *82*, 1147−1152.
(14) Mancinelli, F.; Caraglia, M.; Abbruzzese, A.; d'Ambrosio, G.; Massa, R.; Bismuto, E. Non-thermal Effects of Electromagnetic Fields at Mobile Phone Frequency on the Refolding of an Intracellular Protein: Myoglobin. *J. Cell. Biochem.* **2004**, *93*, 188−196.
(15) Paci, E.; Karplus, M. Unfolding Proteins by External Forces and Temperature: The Importance of Topology and Energetic. *Proc. Natl. Acad. Sci. U.S.A.* **2000**, *97*, 6521−6526.
(16) Paschek, D.; Gnanakaran, S.; Garcia, A. E. Simulations of the Pressure and Temperature Unfolding of an α-Helical Peptide. *Proc. Natl. Acad. Sci. U.S.A.* **2005**, *102*, 6765−6770.

(17) Voelz, V. A.; Bowman, G. R.; Beauchamp, K.; Pande, V. S. Molecular Simulation of *Ab Initio* Protein Folding for a Millisecond Folder NTL9(1−39). *J. Am. Chem. Soc.* **2010**, *132*, 1526−1528.
(18) Li, A.; Daggett, V. Molecular Dynamics Simulation of the Unfolding of Barnase: Characterization of the Major Intermediate. *J. Mol. Biol.* **1998**, *275*, 677−694.
(19) Yin, J.; Bowen, D.; Southerland, W. M. Barnase Thermal Titration via Molecular Dynamics Simulations: Detection of Early Denaturation Sites. *J. Mol. Graphics Modell.* **2006**, *24*, 233−243.
(20) Budi, A.; Legge, S.; Treutlein, H.; Yarovsky, I. Effect of External Stresses on Protein Conformation: A Computer Modelling Study. *Eur. Biophys. J.* **2004**, *33*, 121−129.
(21) Budi, A.; Legge, S.; Treutlein, H.; Yarovsky, I. Electric Field Effects on Insulin Chain-B Conformation. *J. Phys. Chem. B* **2005**, *109*, 22641−22648.
(22) English, N. J.; Mooney, D. A. Denaturation of Hen Egg White Lysozyme in Electromagnetic Fields: A Molecular Dynamics Study. *J. Chem. Phys.* **2007**, *126*, 091105.
(23) English, N. J.; Solomentsev, G. Y.; O'Brien, P. Nonequilibrium Molecular Dynamics Study of Electric and Low-Frequency Microwave Fields on Hen Egg White Lysozyme. *J. Chem. Phys.* **2009**, *131*, 035106.
(24) Solomentsev, G. Y.; English, N. J.; Mooney, D. A. Hydrogen Bond Perturbation in Hen Egg White Lysozyme by External Electromagnetic Fields: A Nonequilibrium Molecular Dynamics Study. *J. Chem. Phys.* **2010**, *133*, 235102.
(25) Roy, D.; Cambre, J. N.; Sumerlin, B. Future Perspectives and Recent Advances in Stimuli Responsive Materials. *Prog. Polym. Sci.* **2010**, *35*, 278−301.
(26) Beebe, S. J.; Schoenbach, K. H. Nanosecond Pulsed Electric Fields: A New Stimulus To Activate Intracellular Signaling. *J. Biomed. Biotechnol.* **2005**, *2005*, 297−300.
(27) Merla, C.; Denzi, A.; Paffi, A.; Casciola, M.; d'Inzeo, G.; Apollonio, F.; Liberti, M. Novel Passive Element Circuits for Microdosimetry of Nanosecond Pulsed Electric Fields. *IEEE Trans. Biomed. Eng.* **2012**, *49*, 2302−2311.
(28) Schoenbach, K. H.; Hargrave, B.; Joshi, R. P.; Kolb, J. F.; Nuccitelli, R.; Osgood, C.; Pakhomov, A.; Stacey, M.; Swanson, R. J.; White, J. A.; Xiao, S.; Zhang, J. Bioelectric Effects of Intense Nanosecond Pulses. *IEEE Trans. Dielectr. Electr. Insul.* **2007**, *14*, 1088−1109.
(29) Hetz, C. The Unfolded Protein Response: Controlling Cell Fate Decisions under ER Stress and Beyond. *Nat. Rev. Mol. Cell Biol.* **2012**, *13*, 89−102.
(30) Scheuner, D.; Kaufman, R. J. The Unfolded Protein Response: A Pathway That Links Insulin Demand with β-Cell Failure and Diabetes. *Endocr. Rev.* **2008**, *29*, 317−333.
(31) Hall, E. H.; Schoenbach, K. H.; Beebe, S. J. Nanosecond Pulsed Electric Fields Induce Apoptosis in p53-Wildtype and p53-Null HCT116 Colon Carcinoma Cells. *Apoptosis* **2007**, *12*, 1721−1731.
(32) Ren, W.; Beebe, S. J. An Apoptosis Targeted Stimulus with Nanosecond Pulsed Electric Fields (nsPEFs) in E4 Squamous Cell Carcinoma. *Apoptosis* **2011**, *16*, 382−393.
(33) Mi, Y.; Yao, C.; Li, C.; Sun, C.; Tang, J.; Yang, F.; Wen, Y. Caspase-3 Activation by Exponential Decay Nanosecond Pulsed Electric Fields on Tumor-Bearing BALB/c Nude Mice in Vivo. *IEEE Trans. Plasma Sci.* **2010**, *38*, 1963−1971.
(34) Breton, M.; Delemotte, L.; Silve, A.; Mir, L. M.; Tarek, M. Transport of siRNA through Lipid Membranes Driven by Nanosecond Electric Pulses: An Experimental and Computational Study. *J. Am. Chem. Soc.* **2012**, *134*, 13938−13941.
(35) Fernandez, M. L.; Risk, M.; Reigada, R.; Vernier, P. T. Size-Controlled Nanopores in Lipid Membranes with Stabilizing Electric Fields. *Biochem. Biophys. Res. Commun.* **2012**, *423*, 325−330.
(36) Austin, R. H.; Beeson, K. W.; Eisenstein, L.; Frauenfelder, H.; Gunsalus, I. C. Dynamics of Ligand Binding to Myoglobin. *Biochemistry* **1975**, *14*, 5355−5373.
(37) Scott, E. E.; Gibson, Q. H.; Olson, J. S. Mapping the Pathways for O2 Entry into and Exit from Myoglobin. *J. Biol. Chem.* **2001**, *276*, 5177−5188.
(38) D'Abramo, M.; Di Nola, A.; Amadei, A. Kinetics of Carbon Monoxide Migration and Binding in Solvated Myoglobin As Revealed by Molecular Dynamics Simulations and Quantum Mechanical Calculations. *J. Phys. Chem. B* **2009**, *113*, 16346−16353.
(39) Aschi, M.; Zazza, C.; Spezia, R.; Bossa, C.; Di Nola, A.; Paci, M.; Amadei, A. Conformational Fluctuations and Electronic Properties in Myoglobin. *J. Comput. Chem.* **2004**, *7*, 974−984.
(40) Tirado-Rives, J.; Jorgensen, W. L. Molecular Dynamics Simulations of the Unfolding of Apomyoglobin in Water. *Biochemistry* **1993**, *32*, 4175−4184.
(41) Apollonio, F.; Libertiaaa, M.; Amadei, A.; Aschi, M.; Pellegrino, M.; D'Alessandro, M.; D'Abramo, M.; Di Nola, A.; d'Inzeo, G. Mixed Quantum-Classical Methods for Molecular Simulations of Biochemical Reactions with Microwave Fields: The Case Study of Myoglobin. *IEEE Trans. Microwave Theory Tech.* **2008**, *56*, 2511−2519.
(42) Hargrove, M. S.; Krzywda, S.; Wilkinson, A. J.; Dou, Y.; Ikeda-Saito, M.; Olson, J. S. Stability of Myoglobin: A Model for the Folding of Heme Proteins? *Biochemistry* **1994**, *33*, 11767−11775.
(43) Geissinger, P.; Kohler, B. E.; Woehl, J. C. Experimental Determination of Internal Electric Fields in Ordered Systems: Myoglobin and Cytochrome *c*. *Synth. Met.* **1997**, *84*, 937−938.
(44) Moczygemba, C.; Guidry, J.; Wittung-Stafshede, P. Heme Orientation Affects Holo-myoglobin Folding and Unfolding Kinetics. *FEBS Lett.* **2000**, *470*, 203−206.
(45) Culbertson, D. S.; Olson, J. S. Role of Heme in the Unfolding and Assembly of Myoglobin. *Biochemistry* **2010**, *49*, 6052−6063.
(46) Nishimura, C.; Dyson, H. J.; Wright, P. E. The Apomyoglobin Folding Pathway Revisited: Structural Heterogeneity in the Kinetic Burst Phase Intermediate. *J. Mol. Biol.* **2002**, *322*, 483−489.
(47) Jamin, M. The Folding Process of Apomyoglobin. *Protein Pept. Lett.* **2005**, *12*, 229−234.
(48) Groot, M.; Vos, M. H.; Schlichting, I.; van Mourik, F.; Joffre, M.; Lambry, J.; Martin, J. Coherent Infrared Emission from Myoglobin Crystals: An Electric Field Measurement. *Proc. Natl. Acad. Sci. U.S.A.* **2002**, *99*, 1323−1328.
(49) Van Der Spoel, D.; Lindahl, E.; Hess, B.; Groenhof, G.; Mark, A. E.; Berendsen, H. J. GROMACS: Fast, Flexible, and Free. *J. Comput. Chem.* **2005**, *26*, 1701−1718.
(50) Berendsen, H. J. C.; Postma, J. P. M.; Gunsteren, W. F. V.;Hermans, J. Interaction Models for Water in Relation to Protein Hydration. In *Intermolecular Forces*, Pullman, B., Ed.; Reidel Publishing Company: Dordrecht, The Netherlands, 1981; pp 331−342.
(51) Berendsen, H. J. C.; Postma, J. P. M.; van Gunsteren, W. F.; Di Nola, A.; Haak, J. R. Molecular Dynamics with Coupling to an External Bath. *J. Chem. Phys.* **1984**, *81*, 3684−3690.
(52) Evans, D. J.; Morriss, G. P. *Statistical Mechanics of Non-equilibrium Liquids*; Academic Press: London, 1990.
(53) Hess, B.; Bekker, H.; Berendsen, H. J. C.; Frajie, J. G. E. M. *J. Comput. Chem.* **1997**, *18*, 1463−1472.
(54) Darden, T. A.; York, D. M.; Pedersen, L. G. *J. Chem. Phys.* **1993**, *98*, 10089.
(55) Van Gunsteren, W. F.; Billeter, S. R.; Eising, A. A.; Hunemberger,P. H.; Kruger, P.; Mark, A. E.; Scott, V. R. P.; Tironi, I. G. *Biomolecular Simulation: The GROMOS96 Manual and User Guide*; Hochschlverlag AG an der ETH: Zurich, Switzerland, 1996.
(56) Kabsch, W.; Sander, C. Dictionary of Protein Secondary Structure: Pattern Recognition of Hydrogen-Bonded and Geometrical Features. *Biopolymers* **1983**, *22*, 2577−2637.